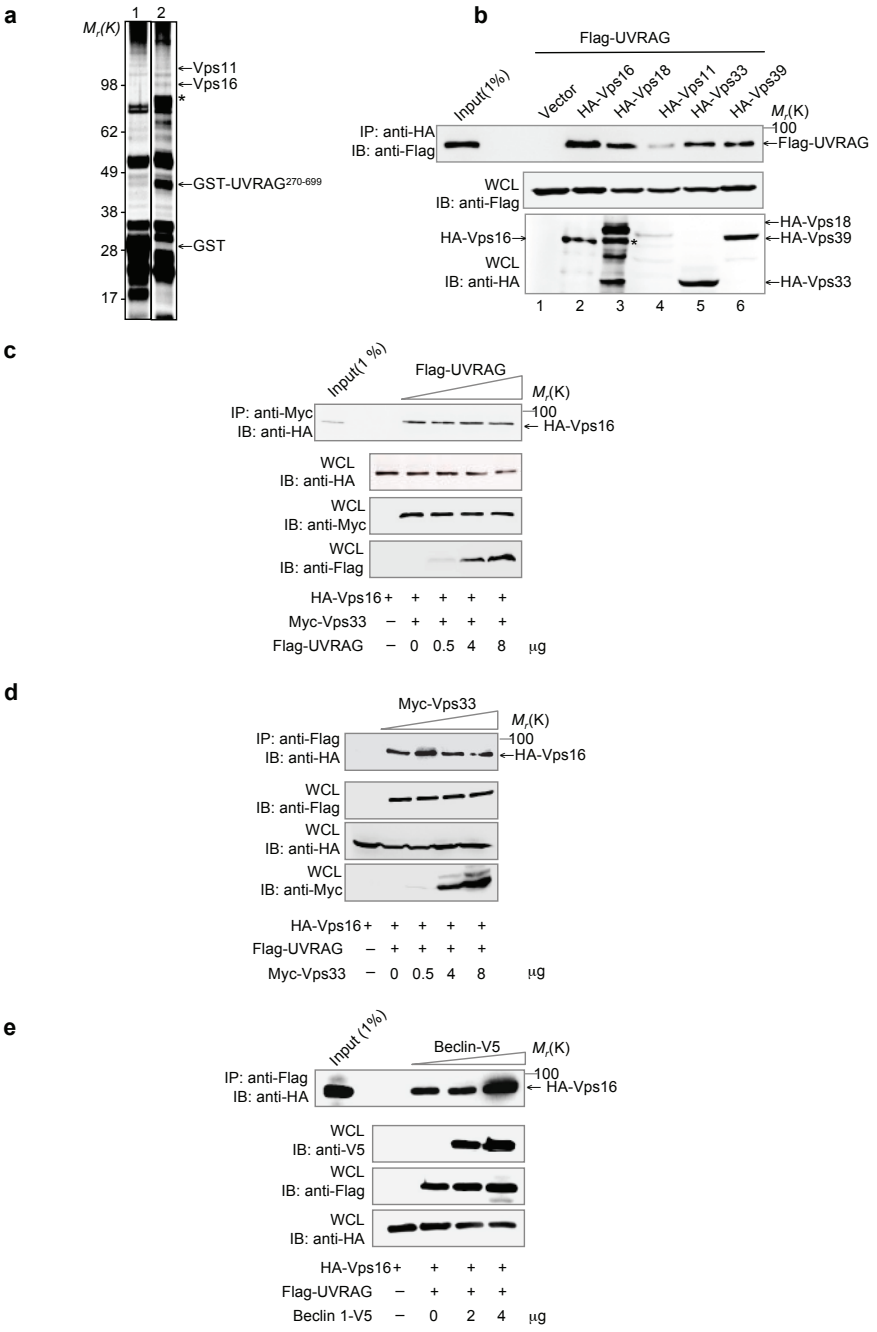

Figure S1 UVRAG interaction with the class C Vps complex. (**a**) UVRAG interacting proteins. After transfection with GST alone (lane 1) or GST-UVRAG$^{270-699}$ (lane 2), 293T cells were used for GST-pulldown and the purified proteins were detected by silver staining. Asterisk indicates the potential contaminating protein(s). Proteins were identified based on mass spectrometry results combined with predicted molecular weights. (**b**) UVRAG interaction with the class C Vps complex subunits. 293T cells were co-transfected with Flag-UVRAG together with empty vector (lane 1), HA-Vps16 (lane 2), HA-Vps18 (lane 3), HA-Vps11 (lane 4), HA-Vps33 (lane 5) or HA-Vps39 (lane 6). Whole-cell lysates (WCLs) were immunoprecipitated (IP) with anti-HA followed by immunoblotting (IB) with anti-Flag. *, protein degradation. (**c**) UVRAG does not compete with Vps33 for Vps16 interaction. 293T cells were transfected with both HA-Vps16 and Myc-Vps33 with increasing amounts of Flag-UVRAG. WCLs were used for co-IP with anti-Myc followed by IB with anti-HA. (**d**) Vps33 does not compete with UVRAG for Vps16 interaction. 293T cells were transfected with both HA-Vps16 and Flag-UVRAG with increasing amounts of Myc-Vps33. WCLs were used for co-IP with anti-Flag followed by IB with anti-HA. (**e**) Beclin1 does not interfere with the interaction between UVRAG and Vps16. 293T cells were transfected with both HA-Vps16 and Flag-UVRAG with increasing amounts of Beclin1-V5. WCLs were used for co-IP with anti-Flag followed by IB with anti-HA. The raw data of the immunoblots in (**b**), (**c**) and (**d**) are shown in the Supplementary Information, Fig. S6.

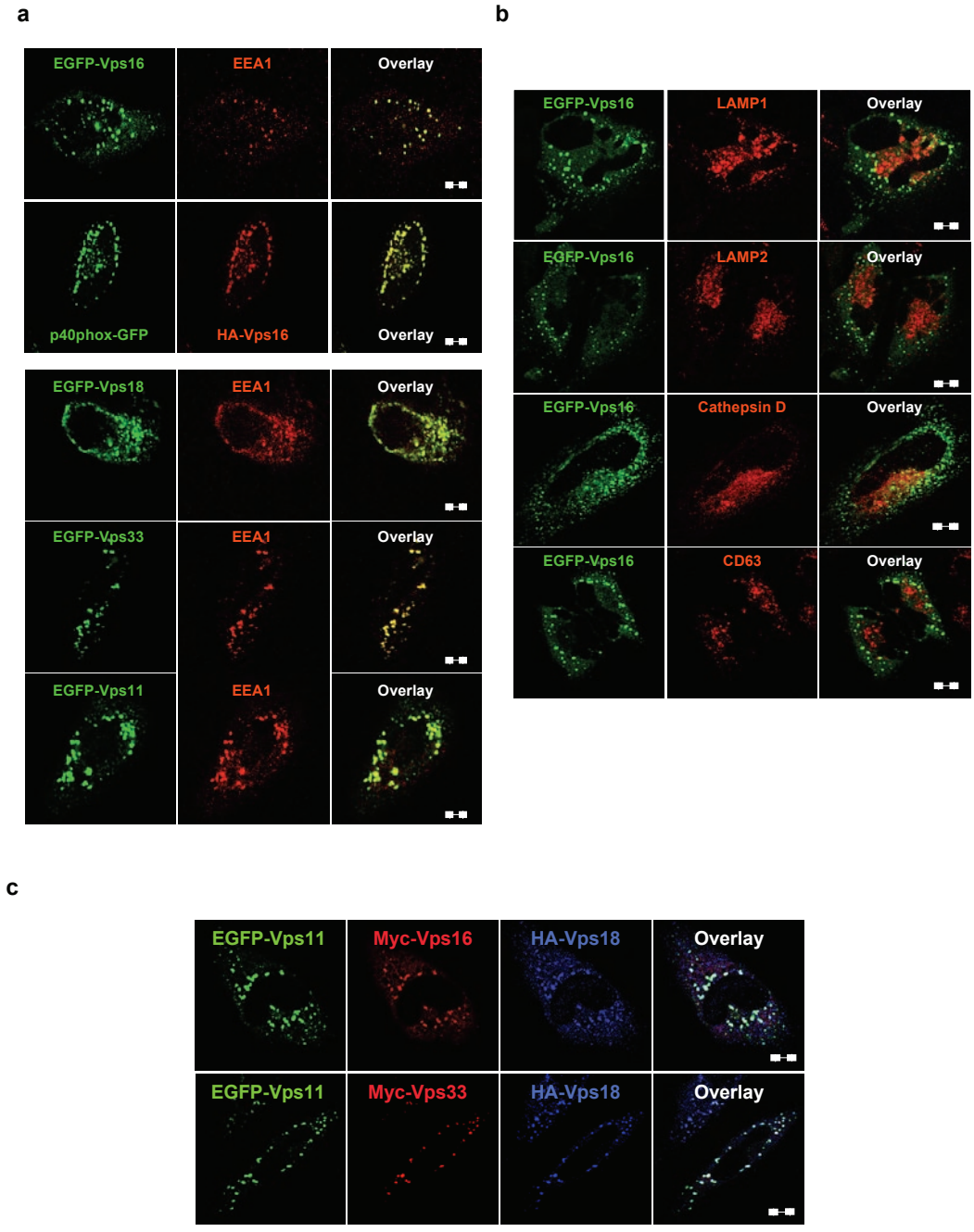

Figure S2 Early endosomal localisation of the class C Vps complex and UVRAG. **(a)** The class C Vps complex subunits localise to early endosomes. HeLa cells were transfected with EGFP-tagged Vps16, Vps18, Vps33 or Vps11 and stained with anti-EEA1 (red) or co-transfected with HA-Vps16 and p40phox-GFP and stained with anti-HA (red), followed by confocal microscopy. Scale bar, 5μm. **(b)** Vps16 does not colocalise with late endosomes. HeLa cells were transfected with EGFP-Vps16 and stained with an antibody specific for either LAMP1, LAMP2, cathepsin D, or CD63. Scale bar, 5μm. **(c)** Colocalisation of the class C Vps complex subunits. HeLa cells were transfected with EGFP-, HA-, and Myc-tagged class C Vps complex subunits and stained with anti-Myc (red) and anti-HA (blue), followed by confocal microscopy. Scale bar, 5μm. **(d)** Early endosomal localisation of UVRAG. Upper panel: HeLa cells were first permeabilised with saponin before fixing, co-stained with anti-UVRAG and anti-EEA1 or anti-Rab5, followed by confocal microscopy. Bottom panel: HeLa cells were transfected with EGFP-UVRAG and stained with anti-TrfR, Rab5, or EEA1, followed by confocal microscopy. Scale bar, 5μm. **(e)** UVRAG does not localise to late endosomes. HeLa cells were transfected with Flag-UVRAG and stained with anti-Flag and anti-LAMP1 (left panel), or transfected with EGFP-UVRAG and stained with anti-CD63 (right panel). Scale bar, 5μm. **(f)** Localisation of UVRAG$^{\Delta N(1-147)}$ mutant to early endosomes. HeLa cells were transfected with the EGFP-UVRAG$^{\Delta N(1-147)}$ mutant and stained with anti-TrfR (red) followed by confocal microscopy. Magnified images (insets) indicate the relative co-localisation of UVRAG$^{\Delta N(1-147)}$ with TrfR. All data in Figure S2 are representative of more than three independent experiments. Scale bar, 5μm.

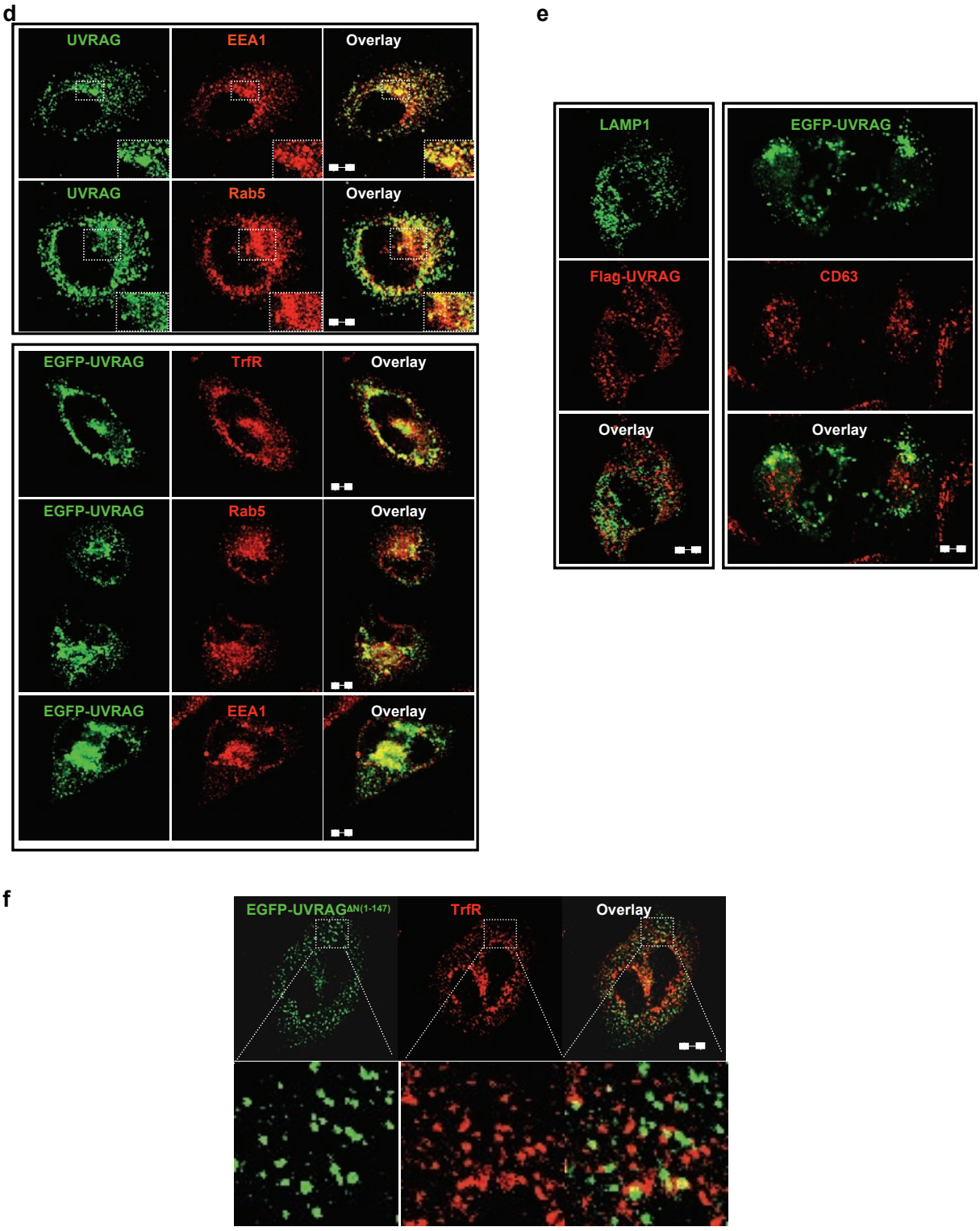

Figure S2 continued

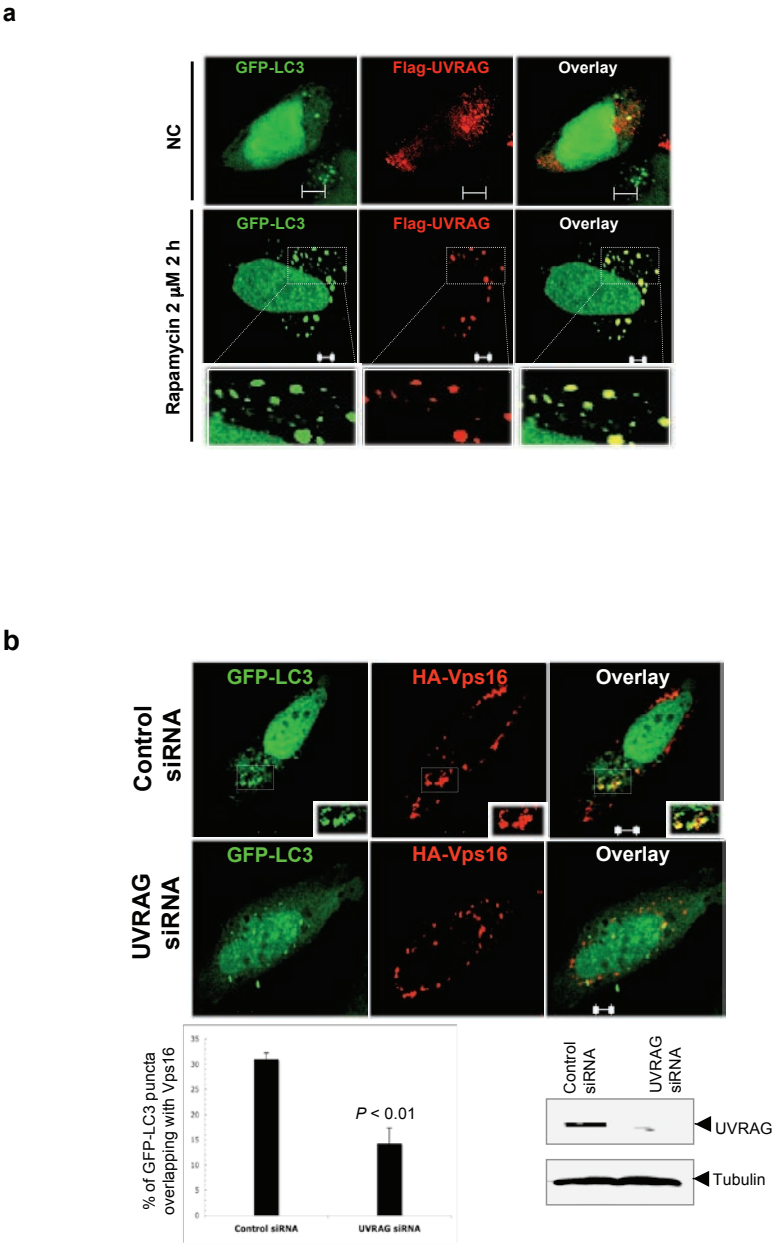

Figure S3 **(a)** Association of UVRAG with autophagosome membranes. HeLa cells were transfected with GFP-LC3 and Flag-UVRAG, incubated either under normal conditions (NC) or treated with 2 μM rapamycin for 2 h. Magnified images (insets) highlight the colocalisation of UVRAG with autophagosomes. Scale bar, 5μm. (**b**) Effects of UVRAG siRNA on Vps16 colocalisation with GFP-LC3. HeLa cells transfected with HA-Vps16 and GFP-LC3 were treated with scrambled siRNA or UVRAG-specific siRNA. Cells were then processed as described in Fig. 3a. Vps16 recruitment to LC3-labeled autophagosomes was analyzed by confocal microscopy (upper panel) and quantified as described in Fig. 3a (lower panel). Scale bars, 5 μm. **(c)** UVRAG enhances the colocalisation efficiency of GFP-LC3 with LAMP1 or LysoTracker Red (LTR) in HCT116 cells. HCT116.Vec and HCT116.UVRAG cells were transfected with GFP-LC3, treated with 2 μM rapamycin, and stained with anti-LAMP or LTR, followed by confocal microscopy. Insets highlight the colocalisation. The percentage of cells with the LAMP1^{+}- and GFP-LC3^{+}-stained autophagosomes was calculated as the mean ± s.e.m. (n = 200) from three independent experiments. Scale bar, 5μm. **(d)** DQ-Red BSA staining of autophagic vacuoles in UVRAG-expressing cells. HCT116.Vec and HCT116.UVRAG cells were transfected with GFP-LC3 and stained with 10 μg ml^{-1} DQ-red BSA for 1 h before fixing, followed by confocal microscopy. Scale bar, 5μm. **(e)** Effect of Beclin1 knockdown on UVRAG-mediated autophagosome formation and maturation. HeLa.Vec and HeLa.UVRAG cells were transfected with GFP-LC3 together with control siRNA or Beclin1 siRNA, followed by confocal microscopy. Arrows in the right bottom panel denote the autophagosomes with LAMP1 staining. IB of Beclin1 and tubulin expression in HeLa.Vec and HeLa.UVRAG cells transfected with control siRNA or Beclin1 siRNA are shown in the upper right panel. The percentage of LAMP1^{+} autophagosomes as well as the number of GFP-LC3-positive dots per cell were calculated and represented as mean ± s.e.m. for combined data from three independent experiments. The raw data of the immunoblots in (**b**) and (**e**) are shown in the Supplementary Information, Fig. S6.

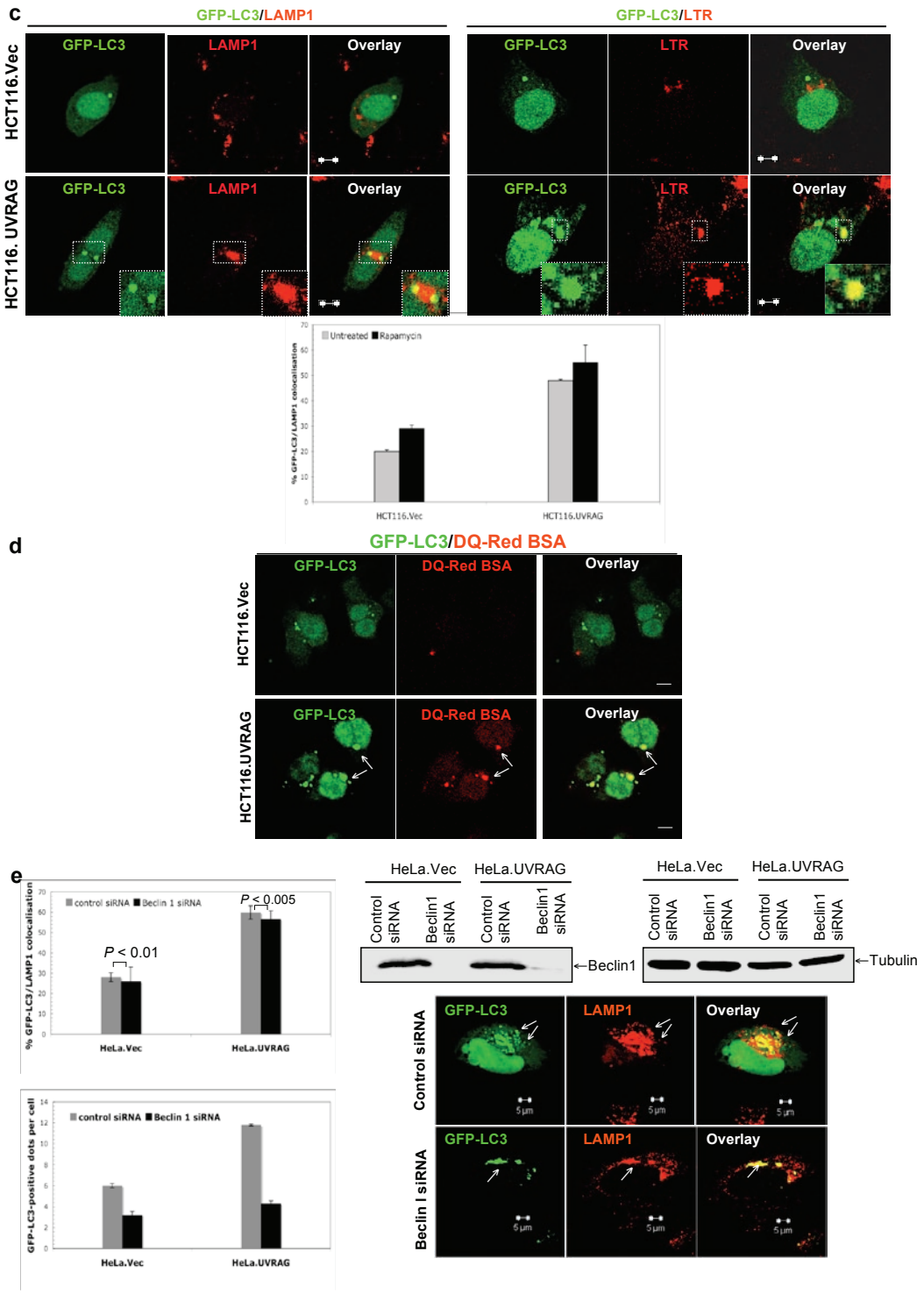

Figure S3 continued

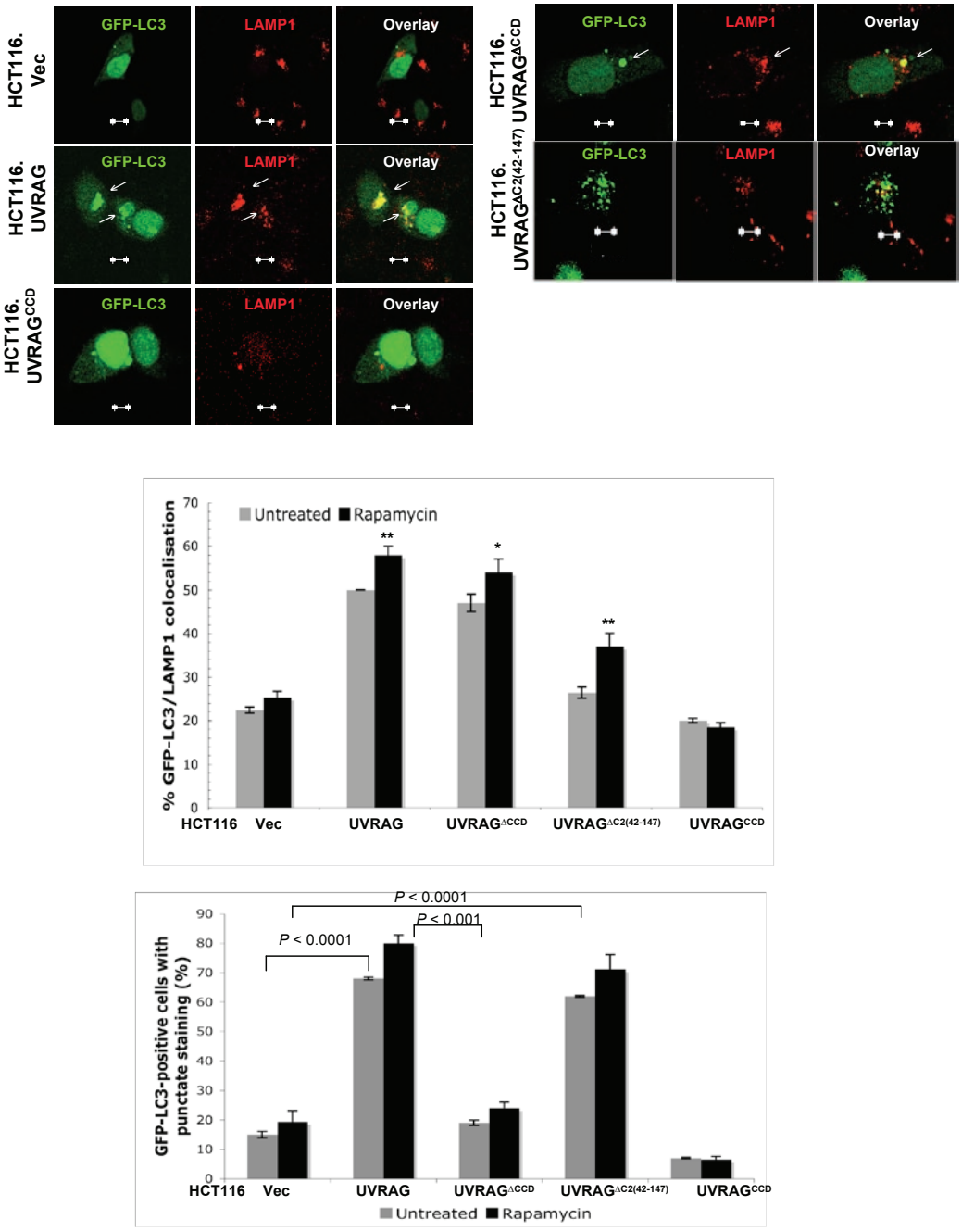

Figure S4 Autophagosome formation and maturation in HCT116 cells stably expressing wt UVRAG or its mutants. HCT116 cells expressing wt UVRAG or its mutants were transfected with GFP-LC3 and treated in the absence or presence of 2 μM rapamycin at 37 °C for 4 h. The LAMP1 staining of GFP-LC3-labeled autophagosomes was analysed by confocal microscopy (upper panel, rapamycin-treated cells) and quantified as the mean ± s.e.m. (n = 300) of results combined from three independent experiments (middle panel). The percentage of GFP-LC3-positive cells with punctate staining was also quantified (bottom panel; mean ± s.e.m.; n = 300). Arrows indicate the colocalised GFP-LC3 with LAMP1 marker. *, $P < 0.01$; **, $P < 0.001$. Scale bars, 5 um.

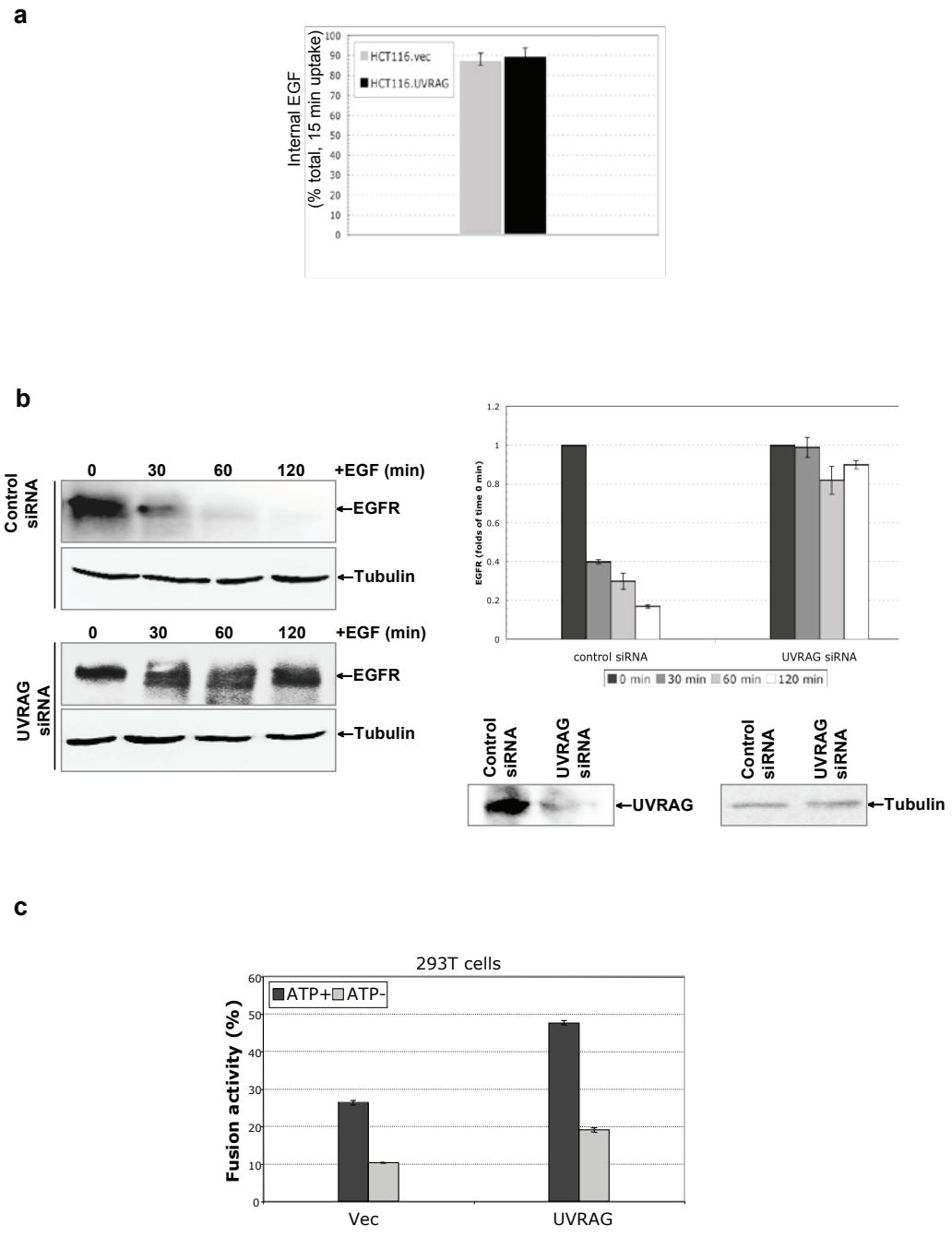

Figure S5 Regulation of endocytic trafficking by UVRAG. **(a)** Uptake of Alexa Fluor–488 EGF. HCT116 cells stably expressing vector or UVRAG were pulse-labeled for 15 min at 37 °C with Alexa Fluor 488–EGF, acid-washed, and lysed. The total amount of fluorescence in the lysate was quantified. Data represent the mean ± s.e.m. for two independent experiments performed in triplicate. **(b)** EGFR degradation in HeLa cells. HeLa cells were transfected with control siRNA or UVRAG siRNA, treated with 200 ng ml^{-1} EGF at 37 °C for the indicated period, and their WCLs were subjected to IB with anti-EGFR (left panel). The EGFR bands at each time point were quantified and indicated as a percentage relative to that at time 0 h (right panel). IB of UVRAG and tubulin expression in HeLa cells transfected with control siRNA or UVRAG siRNA are shown in the bottom right panel. **(c)** Effect of UVRAG on the *in vitro* endosome-endosome fusion. 293T cells transfected with empty vector or Flag-UVRAG were pulse-labeled with avidin-conjugated alkaline phosphatase for 10 min, washed, and chased for 30 min to label late endosomes; or the transfected cells were allowed to internalise biotin-conjugated IgG for 10 min to label early endosomes. Subsequently, cells were lysed and *in vitro* endosome-endosome fusion was performed under standard conditions (see Supplementary Methods for details) in the presence of either an ATP-regenerating system (+ATP) or an ATP-depleting system (–ATP). The data were derived from two representative experiments. The raw data of the immunoblots in (b) are shown in the Supplementary Information, Fig. S6.

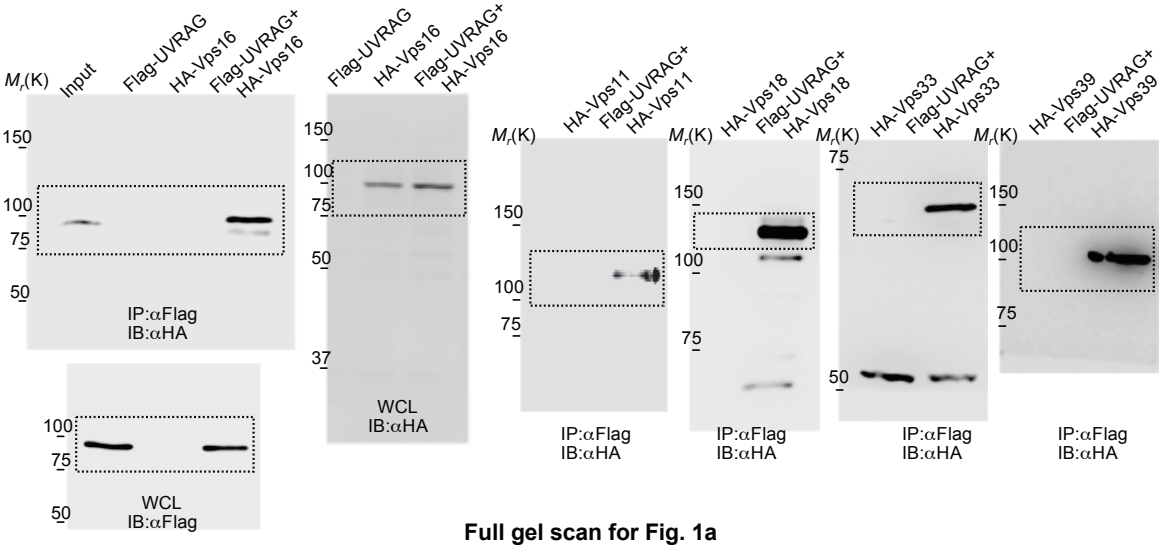

Full gel scan for Fig. 1a

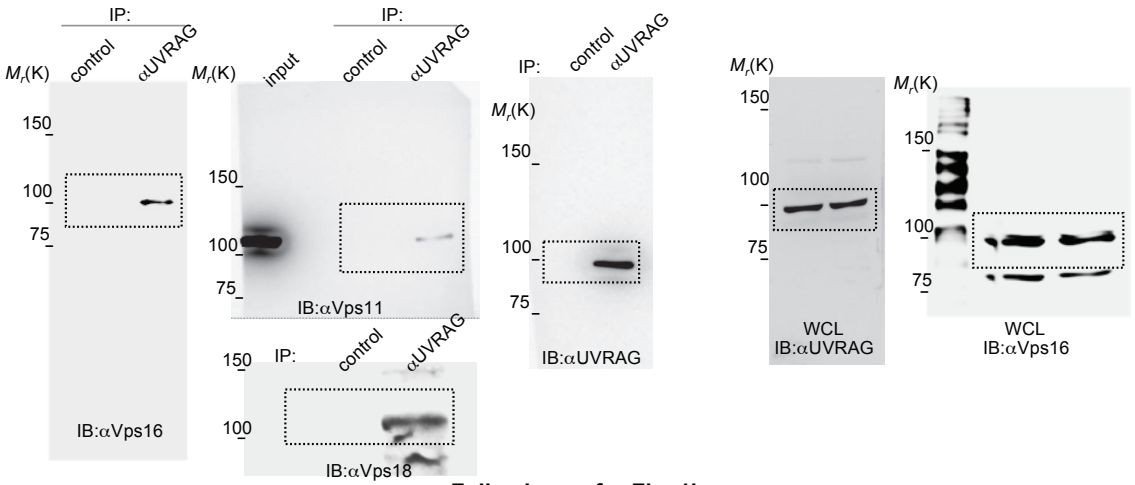

Full gel scan for Fig. 1b

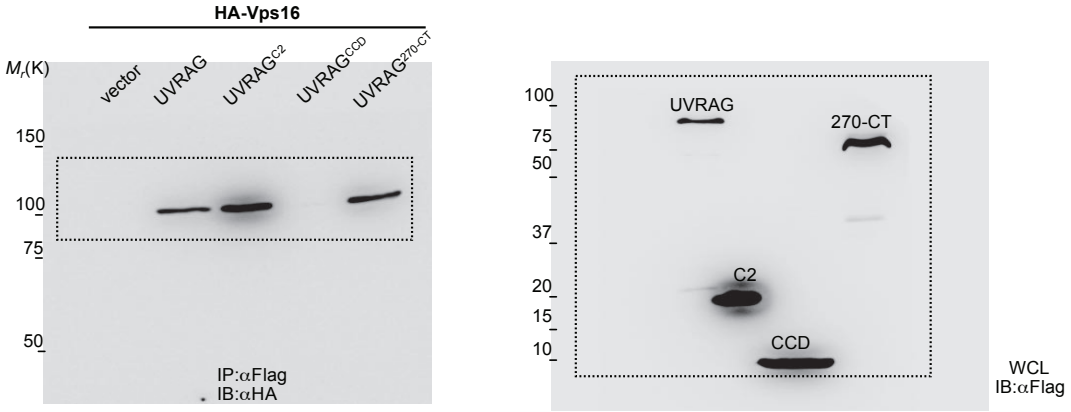

Full gel scan for Fig. 2a

Figure S6 Original gel scan.

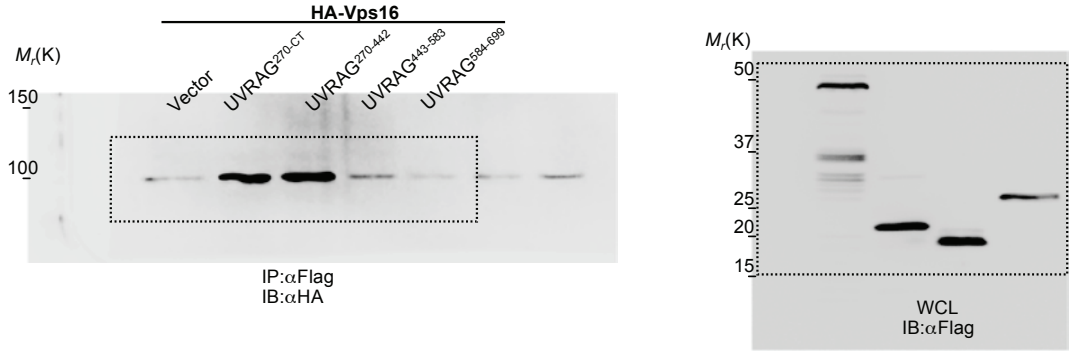

Full gel scan for Fig. 2c

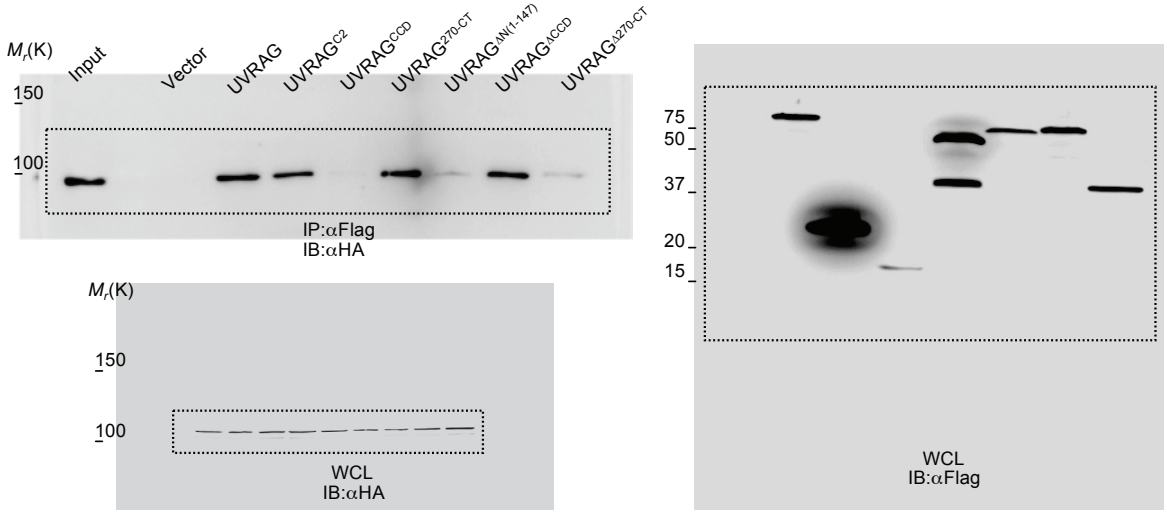

Full gel scan for Fig. 2d

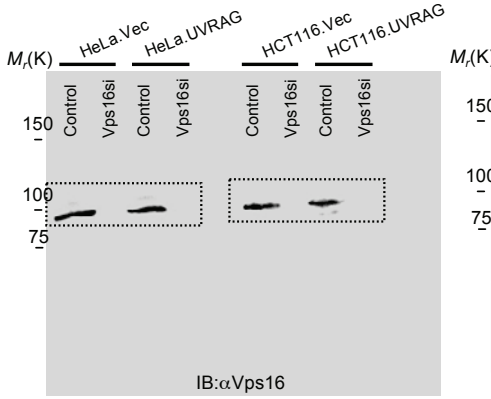

Full gel scan for Fig. 3b

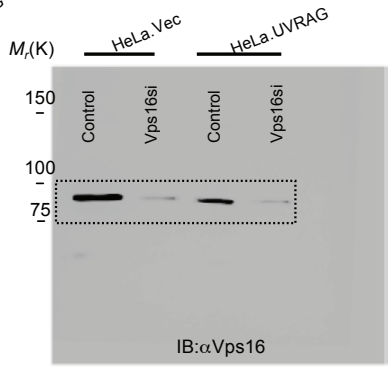

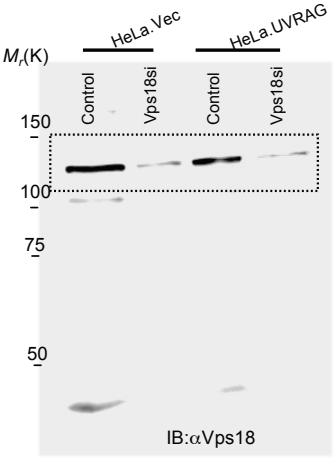

Full gel scan for Fig. 5b

Figure S6 continued

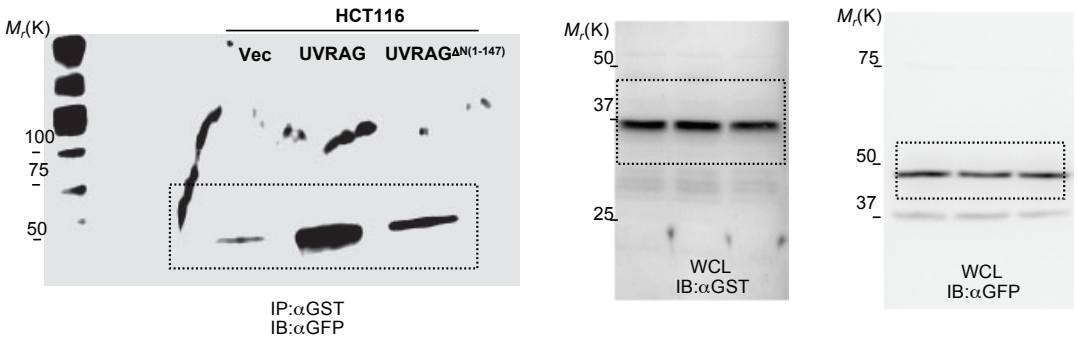

Full gel scan for Fig. 6c

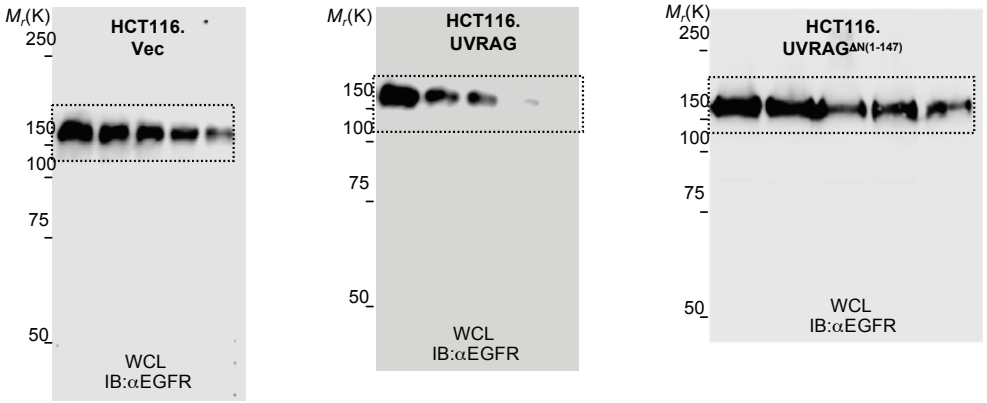

Full gel scan for Fig. 7b

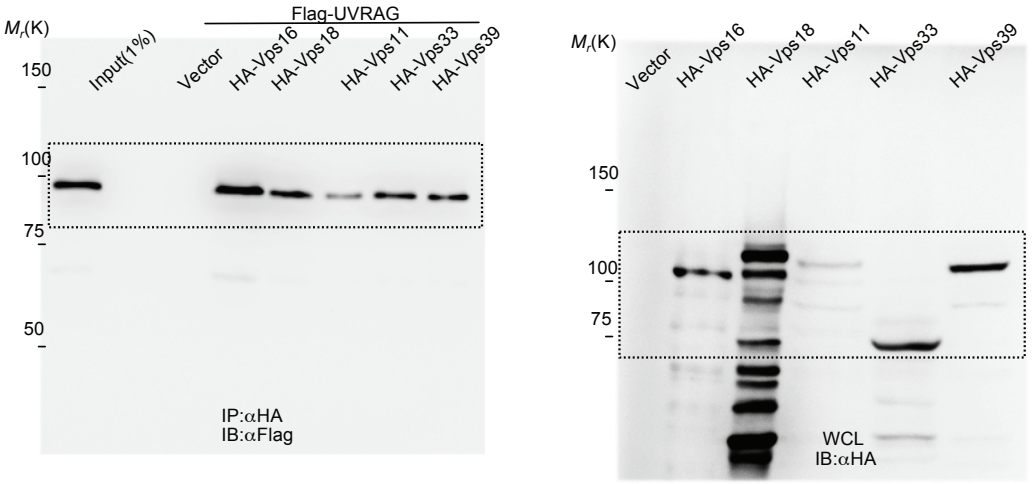

Full gel scan for Fig. S1b

Figure S6 continued

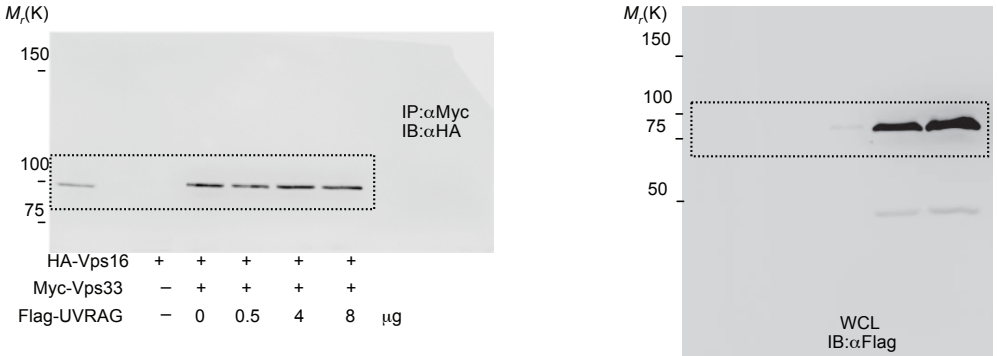

Full gel scan for Fig. S1c

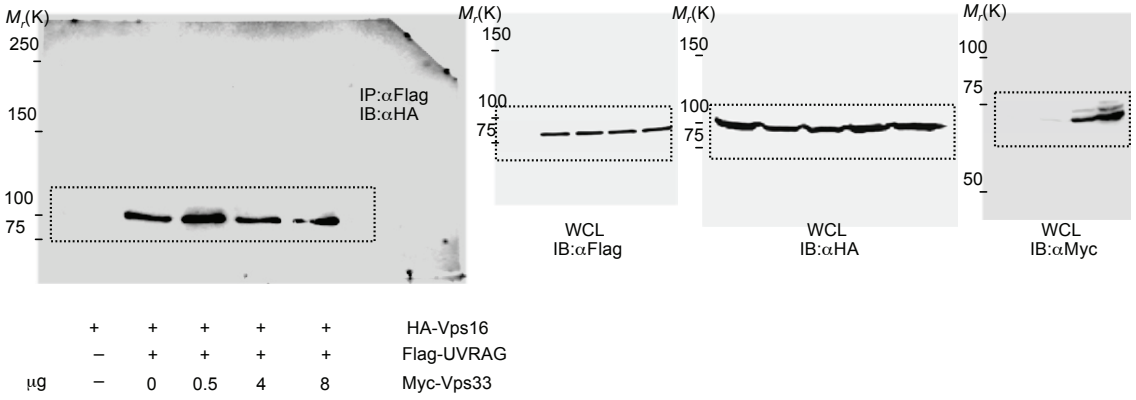

Full gel scan for Fig. S1d

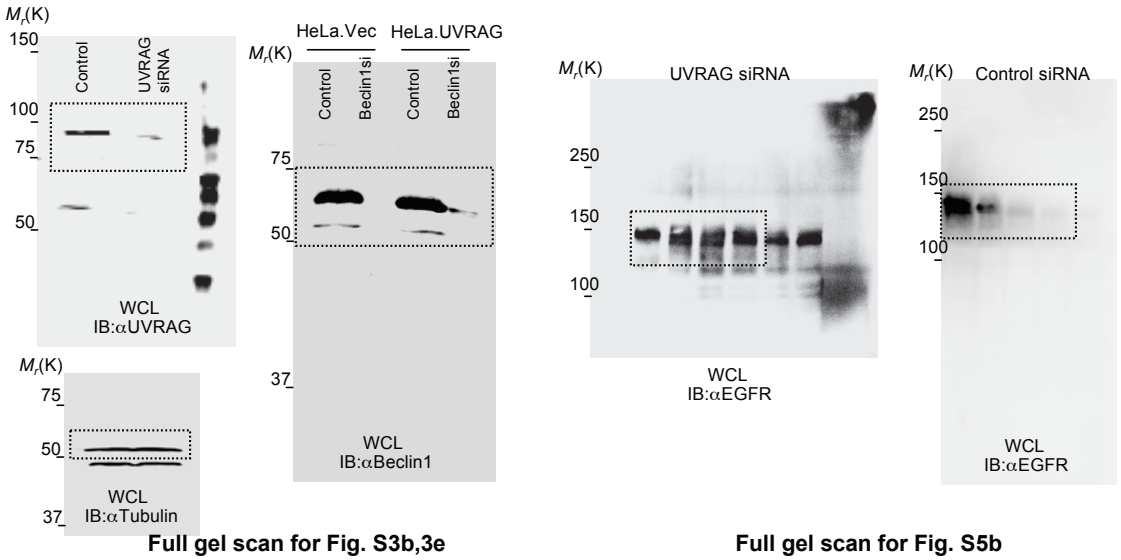

Full gel scan for Fig. S3b,3e **Full gel scan for Fig. S5b**

Figure S6 continued